Preprints of the 21st IFAC World Congress (Virtual)
Berlin, Germany, July 12-17, 2020

Model Based Control with Online Automatic Adaptation by Neural Network for Advanced Diesel Combustion

Jianan Cao* Jihoon Kim* Motoki Takahashi* Yudai Yamasaki*

**The University of Tokyo,7-3-1, Hongo Bunkyo-ku, Tokyo, 113-8656, Japan*
(Tel: 03-5841-6430; e-mail: jkim@fiv.t.u-tokyo.ac.jp).

Abstract: Model based control with physical models are proposed as an alternative to conventional control methods to improve engine performance under real driving conditions including various transient condition. Even if models are built based on physical rules, the models still have several parameters which is desirable to adapt in real time according to driving condition. Therefore, the authors developed an online automatic adaptation method for model-based control of diesel engines, which is based on neural networks. The predictive accuracy of the adapted model has been evaluated by simulation, and the performance of the feed-forward controller based on the model is evaluated by experiment under actual engine.

Keywords: Diesel engine, Model-based control, Automatic adaptation, Neural network.

1. INTRODUCTION

The PCCI (Premixed Charge Compression Ignition) combustion method for diesel engines can be described as an advanced combustion technology that applies the rapid reaction of premixed air and fuel. Due to premixing, the fuel density in PCCI combustion is lean, so the combustion temperature is kept low. Therefore, it can be expected to improve thermal efficiency and suppress NOx, and inhibit the generation of PM as it can avoid fuel richness by premixing. Although PCCI combustion has the advantages mentioned above, its robustness is low due to its high sensitivity to in-cylinder gas composition and gas state. Therefore, the gas state in the cylinder must be considered to stabilize and control ignition and combustion. The in-cylinder gas, however, consists of fresh air, EGR (Exhaust Gas Recirculation) gas, residual gas, etc., and these gasses change depending on operating conditions and ambient conditions. In order to execute PCCI combustion by current map control method based on huge number of experiments, it requires enormous man-hours and costs to consider every gas states one by one.

Also, the RDE (Real Driving Emission) test method where exhaust gas is measured while actual driving on a public road has already been implemented in Europe and other countries such as Japan are also considering to adopt it. As the RDE test method verifies in more complex driving scenes, the range of operation of the engine under evaluation has also been expanded. However, current control maps are constructed considering specific driving modes, and it is difficult to adapt a map that takes into account all actual road driving scenes.

As an alternative to map control, Model-based control has attracted a lot of attention in recent years as a new method of engine control, since this method is expected to implement advanced combustion technology and enhance the performance in various driving scenes. Model-based control in the engine calculates control inputs and executes control in real time by the control model installed in an ECU (Engine Control Unit). As control inputs are calculated in each cycle by the control-oriented model considering operating condition in real time, adequate control can be performed, and improvement of performance in transient operation can therefore be expected.

For the model-based control, the engine control-oriented model can be divided into statistical and physical models. In general, statistical models are based on statistics or system identification (Makowicki *et al.*, 2017), but physical models are built on the basis of the laws of physics (Jade *et al.*, 2015), making them more versatile than statistical models, enabling them to cope with various driving scenes or other engines. Since it is assumed that the control-oriented model is installed in the ECU, considering the specification of the ECU, a control model of a small computational load is required. Ravi et al. have proposed a discretized model of the HCCI engine that expresses in-cylinder pressure history in one cycle by several feature points in one cycle based on physics. This model has a light computational load and is used for the design of controller (Ravi *et al.*, 2010). The authors have developed a discretized model for diesel engines that performs multistage injection by applying the cycle discretization method (Yamasaki *et al.*, 2019a). Also, based on this model, the authors have succeeded in designing and controlling multiple input and multiple output feed-forward controllers in diesel engines (Yamasaki *et al.*, 2019b). Even though the model is based on physics, it has several parameters that need to be adapted. In order to improve control accuracy, it is necessary to adapt these model parameters for each operating condition and engine.

For this purpose, an automatic adjustment method that updates the values of model parameters according to the operating conditions during operation has been studied. A method for adapting model parameters to different driving conditions using a non-linear least square method has been proposed (Grasreiner *et al.*, 2017), but its performance in transient operation has not been validated and online applicability has not been confirmed either. Eguchi et al.

performed online feedback error learning of a FF (Feed-Forward) controller based on a neural network and automatically adapts controller parameters (Eguchi *et al.*, 2018), but the FF controller used is based on neural network and not physics, so the versatility of the controller is weak. The authors proposed online automatic adaptation method by neural network for PCCI combustion control which is based on physical-rich combustion model, its availability was only conducted in simulation (Cao *et al.*, 2019). In addition, recently neural network is paid attention for several application, for engine application such as optimal control of VGT, EGR systems, etc. (Zarghami, *et al.*, 2017; Hu *et al.*, 2019) and its utilization is getting wider.

In this paper, the availability of the model based control system for advanced diesel combustion with our automatic adaptation algorithm based on neural network is evaluated by engine experiment.

Followings are the main contents of this paper. First, experimental set up and control-oriented model for online adaptation are explained. Next, online adaptation algorithm for the control-oriented model based on our previous research is explained and its advantage is validated in simulation. Finally, control experiment by FF controller based on the control-oriented model with the online adaptation algorithm was carried out and its availability was evaluated.

2. EXPERIMENTAL SETUP

The experimental system in this study is same as our previous research (Takahashi *et al.*, 2018). The overall engine system is shown in Fig.1. The engine used in this study is an inline 4-cylinder diesel engine, its displacement is about 2.8L. A common-rail injection system, a variable geometry turbocharger (VGT) and an external exhaust gas recirculation (EGR) system are equipped. A rapid prototyping system (MicroAutoBoxII, dSPACE) with a default ECU is used to measure and control the injection condition and the air path condition. An in-cylinder pressure sensor and a rotary encoder are attached for the analysis of combustion states, and the pressure signal is recorded by a combustion analyser (DS3000, Onosokki) with the pulse of the rotary encoder.

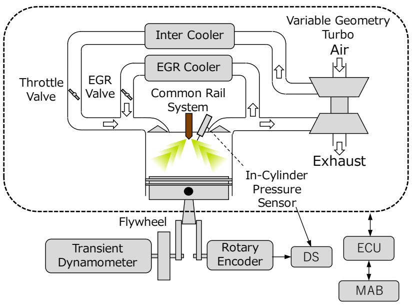

Fig. 1 Engine system (Takahashi *et al.*, 2018)

3. TARGET ENGINE CONTROL MODEL

In this chapter, the control-oriented engine model for automatic adaptation is described. This model has been developed for multiple fuel injections with advanced diesel combustion by the authors and the model is based on physics while including several static models (Yamasaki *et al.*, 2019b). In addition, the model was used as a FF controller, to design a FB controller, and transient operation control succeeded with developed controllers by the test engine. In this paper, the FF controller based on the control oriented model developed by the same concept as our previous works (Yamasaki, *et al.*, 2019 a, b; Takahashi *et al.*, 2019) applying automatic adaptation is installed to the test engine and its availability is evaluated in experiments. The structure of FF controller is shown in chapter 6.

3.1 Model description

The combustion modelled in this paper is a premixed combustion with an injection amount of less than 30 mm^3 per cycle for PCCI combustion, because PCCI combustion is mainly used in low load condition. Fig. 2 shows the history of in-cylinder pressure and heat release rate (HRR) for one cycle of the target combustion. Pilot injection, pre injection, and main injection are executed in one cycle. First HRR peak is the pre HRR peak that appears after pilot injection and pre injection. Second one is the main HRR peak after the main injection. In this type of premixed combustion, high EGR rate results in a long ignition delay, then fuel and air is well mixed before ignition. In addition, when two heat releases, of which interval and peak values, are well controlled, such heat release profiles realize low combustion noise while maintaining high thermal efficiency as well as low emission (Fuyuto *et al.*, 2014).

Instead of predicting a complete histories of in-cylinder pressure and/or heat release rate, only a few features are calculated in the control-oriented engine model. Those feature points are shown as red dots plotted in Fig. 2, and the abbreviation of definitions for the feature points are shown in Table 1.

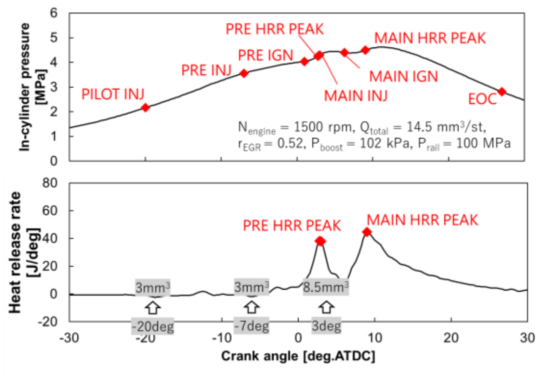

Fig. 2 History of in-cylinder pressure and heat release rate (black lines) and discretized points of the combustion model (red points) (Takahashi *et al.*, 2019)

3.2 Calculation method

This section introduced the calculation method of the control-oriented engine model, especially in ignition and combustion. The mixture gas consisting of intake air, residual gas, and EGR gas is compressed at first, and this process is defined as the polytropic change. Next, ignition and combustion process are calculated considering fuel spray formation, ignition of premixed gas and combustion reaction. Then, expansion

Table 1 Definition of discretized feature points

Discretized point	Definition
IVO	Intake valve open
IVC	Intake valve closing
PILOT INJ	Pilot injection
PRE INJ	Pre injection
PRE IGN	Pre ignition
PRE HRR PEAK	Pre heat release rate peak
MAIN INJ	Main injection
MAIN IGN	Main ignition
MAIN HRR PEAK	Main heat release rate peak
EOC	End of combustion
EVO	Exhaust valve open
EVC	Exhaust valve closing

process is also described as the polytropic change. Finally, gas state at the end of the cycle is taken over as the residual gas to the next cycle, and the gas state at the start of next cycle is predicted in the gas exchange process.

Here, outline of the ignition and the combustion calculation processes are described. The processes include fuel injection, ignition, and combustion reactions and are expressed using a combination of the spray shape model (Reitz and Bracco, 1979), the ignition model (Livengood and Wu, 1955), and the chemical reaction model. In the spray shape model, the spray is considered as a cone shape and its length and angle are expressed as (1) and (2), where, L_{Spray} is the fuel penetration distance, φ_{Spray} is the spray angle, ΔP is the gap between fuel injection pressure and in-cylinder gas pressure, ρ_{Fuel} and ρ_{Gas} are the density of fuel and in-cylinder gas, d_{Hole} is the nozzle hole diameter, t_{Spray} is the injection duration and L_{Nozzle} is the injector nozzle length.

$$L_{Spray} = 2.95\left(\frac{\Delta P}{\rho_{Fuel}}\right)^{0.25}\sqrt{d_{Hole}t_{Spray}} \tag{1}$$

$$\tan(\varphi_{Spray}) = \left\{3.0 + 0.28\left(\frac{L_{Nozzle}}{d_{Hole}}\right)\right\}^{-1} 4\pi\sqrt{\frac{\rho_{Gas}}{\rho_{Fuel}}}\frac{\sqrt{3}}{6} \tag{2}$$

The fuel concentration used in the ignition model and the chemical reaction model can be obtained from the spray shape and amount of injected fuel.

In the ignition model, the ignition delay time is calculated from (3) and (4), which is simplified Livengood and Wu integration for the feature points. Here KA, B, C and E are model parameters to adapt, and Δt_{Delay} is the ignition delay time.

$$\begin{aligned} K &= \int_{INJ}^{IGN}\frac{1}{\tau_{IGN}(t)}dt = \frac{1}{\tau_{IGN}(t_{INJ})}\Delta t_{Delay} \\ &= A[Fuel(t_{INJ})]^{B}[O_2(t_{INJ})]^{C}\exp\left(-\frac{E}{RT(t_{INJ})}\right)\Delta t_{Delay} \end{aligned} \tag{3}$$

$$\begin{aligned} &\Delta t_{Delay} \\ &= KA^{-1}[Fuel(t_{INJ})]^{-B}[O_2(t_{INJ})]^{-C}\exp\left(\frac{E}{RT(t_{INJ})}\right) \end{aligned} \tag{4}$$

The combustion process of the premixed combustion assumes mainly depending on the chemical reaction and the fuel consumption rate is expressed by the Arrhenius equation shown in (5), where, α, β, γ, and ε are also model parameters, and r is the fuel consumption rate. The gas state of each feature point is calculated by the law of energy conservation. Once the ignition timing is determined, the HRR peak timing is predicted by statistical formulas, and the fuel consumption rate is used to calculate the HRR peak value, which are shown in (6), (7).

$$\frac{r}{V_{Fuel}} = \alpha\exp\left(-\frac{\varepsilon}{RT(t_{IGN})}\right)[Fuel(t_{IGN})]^{\beta}[O_2(t_{IGN})]^{\gamma} \tag{5}$$

$$\begin{aligned} &\Delta t_{Peak} \\ &= a_0 + b_0 * \Delta t_{Delay} + c_0 * \frac{n_{Fuel}}{r} + d_0 * P_{rail} + e_0 * r_{EGR} \end{aligned} \tag{6}$$

$$\left.\frac{dQ}{d\theta}\right._{Peak} = a_1 + b_1 * rQ_{LHV} \tag{7}$$

4. AUTOMATIC ADAPTATION METHOD

4.1 Target sub-models

As described in the previous section, model parameters exist in the pre-ignition model and the pre-combustion speed model. In the previous authors' study (Yamasaki *et al.*, 2019a, b), such model parameters were determined by a multiple regression analysis based on data from several steady-state operations, and the results of transient mode control test are shown in Fig. 3. In Fig. 3, black dashed line shows the experimental value, and the blue line shows the prediction result of the model. The prediction accuracy of the combustion model was decreased in the transient operating

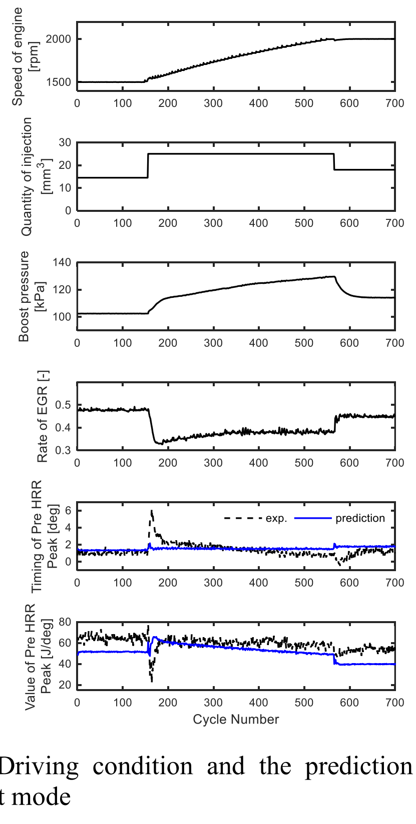

Fig. 3 Driving condition and the prediction result in transient mode

test. Therefore, it is necessary to adapt the model parameters according to each operating condition. So, in this paper, the model and the pre-combustion speed model are adjusted by automatic adaptation method.

4.2 Automatic adaptation algorithm

Automatic adaptation adjusts model parameter values so that the error between the prediction result and the measured value of pre HRR peak becomes zero. As the prediction accuracy of the model gets better, it is expected that the performance of the FF controller based on the model can be improved. In this study, model parameters such as α, β, γ and ε according to the driving conditions are adjusted by neural networks (hereinafter referred to as NN) as automatic adaptation algorithm. By setting driving conditions and model parameters as inputs and outputs of NN, NN becomes a function that represents multiple sets of model parameters as the driving conditions at that time is inputted.

Fig. 4 shows the automatic adaptation flow. First, the driving condition of the cycle is inputted into the NN to update the model parameters. Next, the engine combustion model predicts the state of in-cylinder gas and calculate prediction error. Then, predictive error and loss function is calculated as defined below. Here, $\theta_{Pre\ HRR\ Peak}$ is pre HRR peak timing and $\frac{dQ}{d\theta}_{Pre\ HRR\ Peak}$ is value of pre HRR peak.

$$J = \frac{1}{2}\boldsymbol{u}_{FB,q}^{2} \tag{8}$$

$$\boldsymbol{u}_{FB,q\,1} = \theta_{Pre\ HRR\ Peak\ (model)} - \theta_{Pre\ HRR\ Peak\ (exp.)} \tag{9}$$

$$\boldsymbol{u}_{FB,q\,2} = \frac{dQ}{d\theta}_{Pre\ HRR\ Peak\ (model)} - \frac{dQ}{d\theta}_{Pre\ HRR\ Peak\ (exp.)} \tag{10}$$

Finally, the weight and bias to reduce the loss function by the BP (Back Propagation) method is adjust. Such calculations are performed cycle-by-cycle, so model parameters are updated according to driving conditions in real time. Fig. 5 shows the structure of one node in the NN. Weight and bias are the internal variables of NN. Calculations can be divided into forward and reverse directions. The forward calculation is to get the output from the input and it is written as (11). By applying the BP method, which is written as (12), (13), the prediction error is minimized and the NN weights and biases, and the output, change automatically towards smaller errors.

$$p_{i,j} = F_i\left(w_{i,j}p_{i-1} + b_{i,j}\right), \qquad 1 \le i \le L, 1 \le j \le n_i \tag{11}$$

$$\begin{aligned}\Delta b_L &= \frac{1}{n}\sum_{i=1}^{n}\Delta b_{L,i} = \frac{1}{n}\sum_{i=1}^{n}\frac{\partial J_i}{\partial b_L} = \frac{1}{n}\sum_{i=1}^{n}\frac{\partial J_i}{\partial p_{L,i}}\frac{\partial p_{L,i}}{\partial b_L} \\ &= \frac{1}{n}\sum_{i=1}^{n} W_{out}^{\mathrm{T}}\Delta b_{out} \odot f_L\left(W_L p_{L-1,i} + b_L\right)\end{aligned} \tag{12}$$

$$\begin{aligned}\Delta W_L &= \frac{1}{n}\sum_{i=1}^{n}\Delta W = \frac{1}{n}\sum_{i=1}^{n}\frac{\partial J_i}{\partial W_L} = \frac{1}{n}\sum_{i=1}^{n}\frac{\partial J_i}{\partial p_{L,i}}\frac{\partial p_{L,i}}{\partial W_L} \\ &= \frac{1}{n}\sum_{i=1}^{n}\left\{W_{out}^{\mathrm{T}}\Delta b_{out} \odot f_L\left(W_L p_{L-1,i} + b_L\right)\right\} p_{L-1,i}^{\mathrm{T}} \\ &= \frac{1}{n}\sum_{i=1}^{n}\Delta b_{L,i} p_{L-1,i}^{\mathrm{T}}\end{aligned} \tag{13}$$

In this paper, two NNs were built and the structure of the neural networks were modified from the previous research (Cao, J. *et al.*, 2019) to improve simulation and control performance. First, the number of hidden layers were changed from two to one. This is because in the case of two hidden layers, the vanishing gradient problem has occurred in the NN.

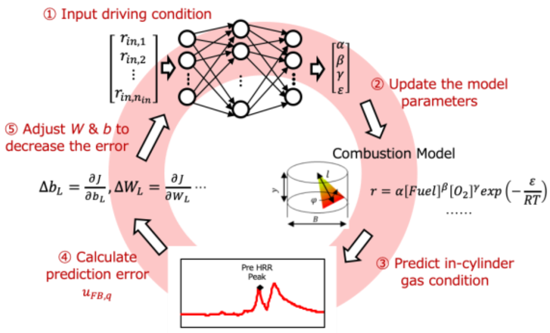

Fig. 4 Automatic adaptation flow (Cao *et al.*, 2019)

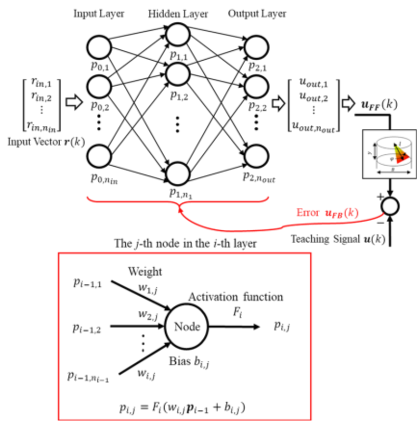

Fig. 5 The outline of the neural network

Moreover, the training speed was faster and the predictive accuracy was higher for one hidden layer than for two hidden layers in the simulation results. Second, the output layer activation function of the pre-ignition model has been changed from a linear activation function to a standard sigmoid function considering expressivity. By changing the activation function, the simulation results improved and were also stable in the control test. Their specifications of NNs are shown in Table 2. Since the premixed fuel and air conditions have significant effect on combustion, the engine speed, total fuel injection quantity, supercharging pressure, and EGR rate

Table 2 Specifications of neural networks

Object model	Input	Output	Number of nodes	Activation function
Pre Ignition Model	N_{Engine} Q_{Total} P_{Boost} r_{EGR}	$(KA)_{PRE}$ B_{PRE} C_{PRE} E_{PRE}	[4,20,4]	Sigmoid function
Pre Combustion Speed Model		α_{PRE} β_{PRE} γ_{PRE} ε_{PRE}		

are used as NN inputs. Both NNs are 4-input 4-output NN with one hidden layer, and there are 20 nodes in a hidden layer. NNs are used to adapt the pre-ignition model and pre-combustion speed model. A standard sigmoid function is the activation function of the hidden and output layers.

5. AUTOMATIC ADAPATION IN SIMULATION

In this chapter, the automatic adaptation of the control-oriented model is performed in simulation before applying the model to the real engine as a FF controller. The automatic adaptation simulation is implemented with experimental data which is collected under the driving condition which is shown in Fig. 6. The simulation environment is MATLAB® and Simulink® (MathWorks, Inc. registered trademark). In the simulation, experimental values of pre HRR timing and pre HRR value were given to NN cycle by cycle. The process of sequentially applying the data from the beginning to the end of this driving pattern to the NN is defined as one time of learning. Before the learning begins, the weight and bias of the NNs is adjusted so that the NNs can output model parameters whose value is close to the conventional ones derived by multiple regression analysis. Fig. 7 shows the prediction result of the models after 500 learnings. The black dashed line is the measured value from the actual engine, which is the target value of the automatic adaptation algorithm. The blue solid line shows the result of using fixed model parameters adapted by multiple regression analysis. The red solid line indicates the result when automatic adaptation is applied. The model with automatic adaptation performs better in both predictions compared to the conventional model, particularly in accelerating operation in about 160~580th cycle. In steady state driving in 1~160th cycle and 580~700th cycle, the conventional model predicts pre HRR timing slightly better than the automatic adaptation model, but in the prediction of pre HRR value, the accuracy of the automatic adaptation model is better. However, there are some cycles where the prediction results are bad. In around 150~160th cycle, the red line goes the opposite of the black dashed line in both two predictions. This is because the data of the transient in 150~160th cycle is quite little compared to other driving condition. Also the in-cylinder gas state of the transient in 150~160th cycle should be pretty different with other cycle, considering it is immediately after a significant increase of injection quantity. For these reasons, the data in 150~160th cycle is not fully learned, hence the accuracy drops.

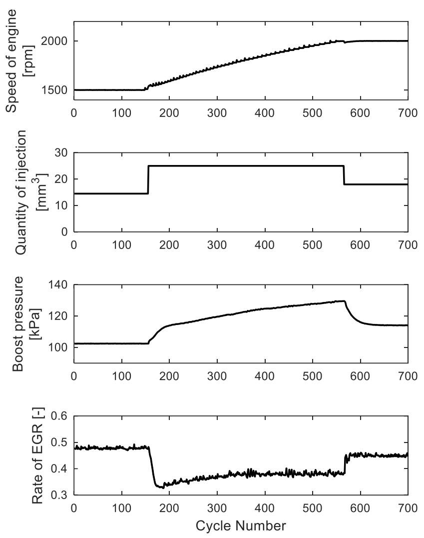

Fig. 6 Driving condition for automatic adaptation in simulation

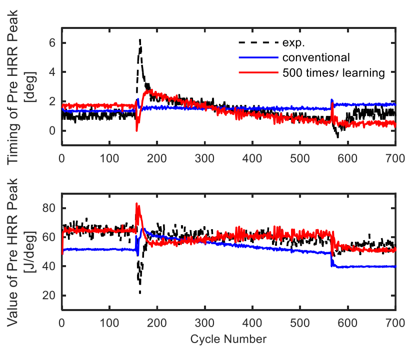

Fig. 7 Prediction result of the models after 500 learnings

Fig. 8 shows the model's prediction accuracy (RMSE) for the learning time. The horizontal axis indicates the time of learnings, and the vertical axis indicates the RMSE of the prediction result. In every 50 times of learnings, RMSE is calculated with the same driving pattern. This figure shows that the prediction accuracy of the automatic adaptation model gets better than the conventional model after 50 times' learning, and it continues to improve as the number of

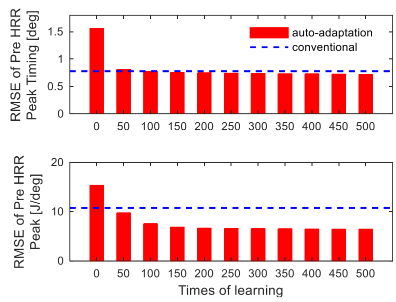

Fig. 8 Prediction accuracy of the automatic adaptation model in simulation

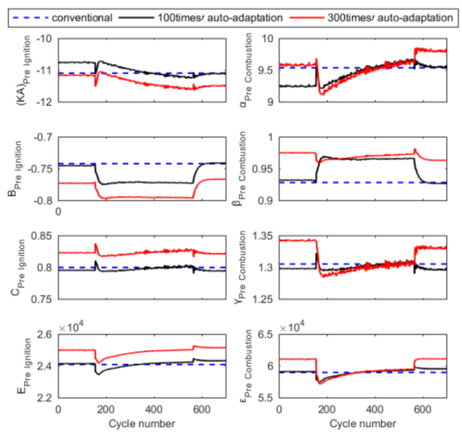

Fig. 9 History of the model parameters in simulation

learning increases. The history of model parameter is shown in Fig. 9. The blue dashed lines are the fixed model parameters adapted by multiple regression analysis, and black and red lines are values of parameters after 100 and 300 times of learning. Fig. 9 shows model parameters changing according to the operating conditions in real time.

6. CONTROL EXPERIMENT

In this chapter, the result of the control experiment is introduced. First, the design of the (FF) controller is described. Next, the FF controller with automatic adaptation algorithm is installed to the rapid prototyping and control experiment was carried out.

6.1 The design of the FF controller

By using the model introduced in chapter 3, the feed-forward (FF) controller is designed and the control system is shown in Fig. 10. The FF controller consists of two parts, an inverse model and a compensator for errors produced by linearization.

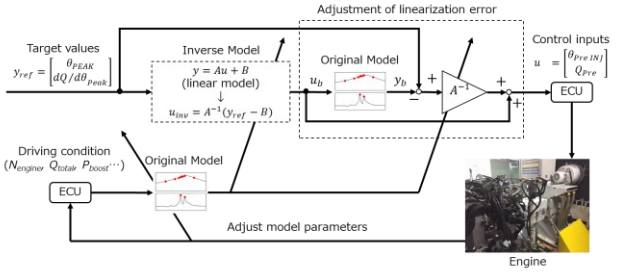

Fig. 10 Block diagram of feed-forward control system

As the model is made up of many equations, it is difficult to obtain an inverse model analytically. Linearization procedure using relation between perturbed input and output is introduced. After the model parameters are updated, the calculation is executed several times when the input is perturbed under the current operating condition $\mathbf{u_d}$. The calculation is performed three times for each input, so the number of calculations is 3^{n}, where n is the amount of input and output. The linear model $\mathbf{y} = \mathbf{Au} + \mathbf{B}$ can be obtained from the output response, and the inverse model is derived by multiplying $\mathbf{A^{-1}}$. In addition, since the combustion model has nonlinearity, an error may arise from the above linearization method and the compensator for occurred error is set. The control input $\mathbf{u_b}$ (in this study, the timing and the quantity of pre injection) derived from the inverse model is inputted again into the original combustion model and the predicted result $\mathbf{y_b}$ (in this study, pre HRR peak timing and value) is calculated. The difference between the predicted result $\mathbf{y_b}$ and the target value $\mathbf{y_{ref}}$ is multiplied by the inverse model coefficient matrix $\mathbf{A^{-1}}$ to obtain the input correction. The above process is executed in every cycle.

6.2 Control experiment result

We noticed that the model parameters are very sensitive because they are power or exponential in the target models. Although it is desirable to set limit or saturation to ensure the stability of the control system, in this research, it is difficult because like the model parameter value, the value of limit or saturation cannot be found in physical way. To solve this problem, while keeping the driving condition the same as shown in Fig. 6, we collect data where various pre injection patterns, including the lower and the upper limit of pre injection timing and quantity, are applied. In that way, the over-learning can be avoided, which means the accuracy of the model could be improved in not only just one certain injection pattern but also various conditions, hence the stability of the controller is improved.

The control experiment is performed with the model parameter obtained in simulation using the data mentioned in last paragraph. The test condition and the result are shown in Fig. 11. In this test, online learning is not conducted while

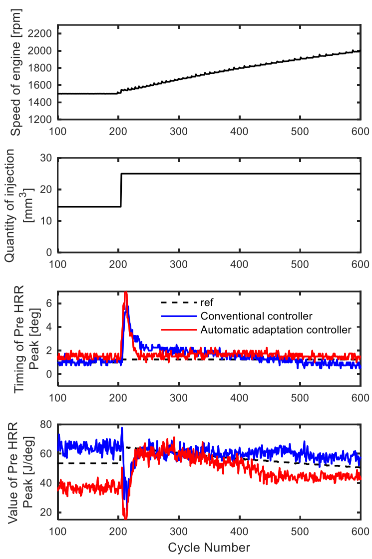

Fig. 11 Driving condition and result in the control test without online learning

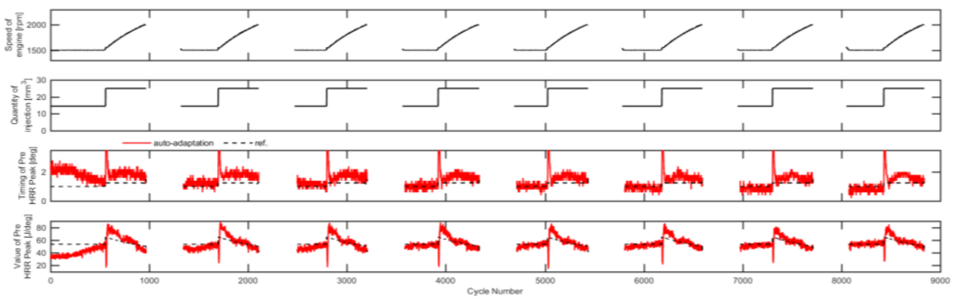

Fig. 12 Driving condition and result in the control test with online learning

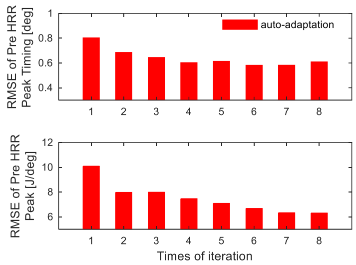

Fig. 13 Prediction accuracy of the automatic adaptation

executing control. The black line refers to the control target, the blue line is the result of the conventional controller which model parameters are adapted by multiple regression analysis, and the red line is the result of the automatic adaptation controller. The figure shows that the control accuracy of the automatic adaptation controller cannot be better than the conventional one by only using the model parameters obtained from simulation. Next, the control experiment is executed while the learning is being conducted. The driving pattern shown in Fig. 11 is repeated for eight times, and how control accuracy changes as the time of repetition increases is observed, which is shown in Fig. 12. The black dashed line refers to the target of control, the red line is the result of the automatic adaptation controller. The control accuracy expressed by RMSE is shown in Fig. 13. Overall, as the learning time of the repetition increases, the control accuracy gets better and better. The control accuracy of pre HRR timing gets a little worse in the 5th and the 8th repetition, which is considered to be caused by the fluctuation of the weight and bias of the NN.

7. CONCLUSIONS

In this paper, the authors developed an online automatic adaptation method for model-based control of diesel engines. An automatic adaptation method based on neural networks has been developed to adapt the model parameters existing in a control-oriented physically rich combustion model. The prediction accuracy of the automatic adaptation model was evaluated by simulation. In addition, availability of the automatic adaptation model as the FF controller was evaluated by experiment. The proposed method is able to improve the prediction accuracy of the engine control model, then improve the control accuracy of the FF controller based on the model. Also, the calculation load of the controller is light enough to conduct on actual engine with the rapid prototyping system. However, the stability of the control system still needs improvement as the future work.

ACKNOWLEDGEMENTS

This paper is the result of a collaborative research program with the Research association of Automotive Internal Combustion Engines (AICE) for fiscal year 2019-2020. The authors gratefully acknowledge the concerned personnel.

REFERENCES

Cao, J., Takahashi, M., Yamasaki, Y., and Kaneko, S. (2019). Online automatic adaptation for model-based control of diesel engine. *Powertrains, Fuels & Lubricants*, JSAE20199184 / SAE2019-01-2320.

Eguchi, M., Mengxing, Q., Ohmori, H., Yamasaki, Y., and Kaneko, S. (2018). Diesel engine combustion control using feedback error learning with artificial intelligence feedforward controller. *Transactions of Society of Automotive Engineers of Japan*, 49(2), 230-234.

Fuyuto, T., Taki, M., Ueda, R., Hattori, Y., Kuzuyama, H., and Umehara, T. (2014). Noise and Emissions Reduction by Second Injection in Diesel PCCI Combustion with Split Injection. *SAE International Journal of Engines*, 7(4), 1900-1910.

Grasreiner, S., Neumann, J., Wensing, M., and Hasse, C. (2017). Model-based virtual engine calibration with the help of phenomenological methods for spark-ignited engines. *Applied Thermal Engineering*, 121, 190-199.

Hu, B., Yang, J., Li, J., Li, S. and Bai, H. (2019). Intelligent Control Strategy for Transient Response of a Variable Geometry Turbocharger System Based on Deep Reinforcement Learning. *Processes*, 7(9), 601.

Jade, S., Larimore, J., Hellström, E., Stefanopoulou, A. G., and Jiang, L. (2015). Controlled Load and Speed Transitions in a Multi cylinder Recompression HCCI Engine. *IEEE Transactions on Control Systems Technology*, 23(3), 868-881.

Livengood, J. C. and Wu, P. C. (1955). Correlation of autoignition phenomena in internal combustion engines and rapid compression machines. *Symposium (International) on Combustion*, 5(1), 347-355.

Makowicki, T., Bitzer, M., Grodde, S., and Graichen, K. (2017). Cycle-by-Cycle Optimization of the Combustion during Transient Engine Operation. *IFAC-PapersOnLine*, 50(1), 11046-11051.

Ravi, N., Jungkunz, A. F., Roelle, M. J. and Gerdes, J. C. (2010). Model-based control of HCCI engines using exhaust recompression. *IEEE Transactions on Control Systems Technology*, 18(6), 1289-1302.

Reitz, R.D, and Bracco, F.B. (1979). On the dependence of spray parameters on nozzle design and operating conditions. *SAE technical paper* 790494.

Takahashi M., Yamasaki Y., Kaneko S., Koizumi J., Hayashi T. and Hirata M. (2018). Model-Based Control System for Air Path and Premixed Combustion of Diesel Engine. *IFAC-PapersOnLine*, 51(31), 522-528.

Takahashi M., Yamasaki Y., Kaneko S., Fujii S., Mizumoto I., Hayashi T. and Hirata M. (2019). Model-based control system for a diesel engine. *IFAC-PapersOnLine*, 52(5), 171-177.

Yamasaki, Y., Ikemura, R., Shimizu, F., and Kaneko, S. (2019a). Simple combustion model for a diesel engine with multiple fuel injections. *International Journal of Engine Research*, 20(2), 167-180.

Yamasaki, Y., Ikemura, R., Takahashi, M., Kaneko, S., and Uemichi, A. (2019b). Multiple-input multiple-output control of diesel combustion using a control-oriented model. *International Journal of Engine Research*, 20(10), 1005-1016.

Zarghami, M., Hosseinnia, S. H. and Babazadeh, M. (2017). Optimal Control of EGR System in Gasoline Engine Based on Gaussian Process. *IFAC-PapersOnLine*, 50(1), 3750-3755.